

A physically based estimate of radiative forcing by anthropogenic sulfate aerosol

Steven J. Ghan,¹ Richard C. Easter,¹ Elaine G. Chapman,¹ Hayder Abdul-Razzak,² Yang Zhang,³ L. Ruby Leung,¹ Nels S. Laulainen,¹ Rick D. Saylor,⁴ and Rahul A. Zaveri¹

Abstract. Estimates of direct and indirect radiative forcing by anthropogenic sulfate aerosols from an integrated global aerosol and climate modeling system are presented. A detailed global tropospheric chemistry and aerosol model that predicts concentrations of oxidants as well as aerosols and aerosol precursors, is coupled to a general circulation model that predicts both cloud water mass and cloud droplet number. Both number and mass of several externally mixed aerosol size modes are predicted, with internal mixing assumed for the different aerosol components within each mode. Predicted aerosol species include sulfate, organic and black carbon, soil dust, and sea salt. The models use physically based treatments of aerosol radiative properties (including dependence on relative humidity) and aerosol activation as cloud condensation nuclei. Parallel simulations with and without anthropogenic sulfate aerosol are performed for a global domain. The global and annual mean direct and indirect radiative forcing due to anthropogenic sulfate are estimated to be -0.3 to -0.5 and -1.5 to -3.0 W m^{-2} , respectively. The radiative forcing is sensitive to the model's horizontal resolution, the use of predicted versus analyzed relative humidity, the prediction versus diagnosis of aerosol number and droplet number, and the parameterization of droplet collision/coalescence. About half of the indirect radiative forcing is due to changes in droplet radius and half to increased cloud liquid water.

1. Introduction

Most of the uncertainty in estimates of anthropogenic forcing of climate change is in the estimates of forcing by anthropogenic aerosols [Intergovernmental Panel on Climate Change (IPCC), 1995]. In the global mean the present-day radiative forcing by anthropogenic greenhouse gases is estimated to be 2.1 – 2.8 W m^{-2} ; the direct forcing by anthropogenic aerosols is estimated to be -0.3 to -1.5 W m^{-2} , while the indirect forcing by anthropogenic aerosols is estimated to be 0 to -1.5 W m^{-2} . Given the uncertainty in the estimates of each radiative forcing component, estimates of the total global mean present-day anthropogenic forcing range from 3 W m^{-2} to -1 W m^{-2} . Clearly, the great uncertainty in the radiative forcing must be reduced if the observed climate record is to be reconciled with model predictions and if estimates of future climate change are to be useful in formulating emission policies. Doing so will require profound reductions in the uncertainties of direct and indirect forcing by anthropogenic aerosol.

How can the uncertainty in anthropogenic aerosol forcing be reduced? Penner *et al.* [1994] and the National Research Council (NRC) [1996] Panel on Aerosol Radiative Forcing and Climate Change describe a strategy for reducing the uncertainty. It consists of a combination of process studies designed to improve understanding of the key processes involved in the forcing, closure experiments designed to evaluate that understanding, and integrated models that treat all of the necessary processes together and estimate the forcing. This paper describes the application of such an integrated model to the estimate of the radiative forcing by anthropogenic sulfate aerosol.

The integrated model is called MIRAGE (Model for Integrated Research on Atmospheric Global Exchanges). It consists of a detailed global tropospheric chemistry and aerosol model that predicts concentrations of oxidants as well as aerosols and aerosol precursors, coupled to a general circulation model that predicts cloud water and cloud ice mass and cloud droplet and ice crystal number concentrations [Ghan *et al.*, 1997a,b]. Both number and mass of several externally mixed lognormal aerosol size modes are predicted, with internal mixing assumed for the different aerosol components within each mode. Predicted aerosol species include sulfate, organic and black carbon, nitrate, soil dust, and sea salt. The models use physically based treatments of aerosol radiative properties (including dependence on relative humidity) and aerosol activation as cloud condensation nuclei. R. C. Easter *et al.* (manuscript in preparation; 2000) (hereinafter referred to as E2000) describe the treatment of chemistry and aerosol physics and evaluate the simulation of the aerosol and aerosol precursors in MIRAGE. Ghan *et al.* [this issue (a, b)] describe

¹Pacific Northwest National Laboratory, Richland, Washington.

²Texas A&M University, Kingsville, Texas.

³Atmospheric and Environmental Research, San Ramon, California.

⁴Georgia Institute of Technology, Atlanta.

Copyright 2001 by the American Geophysical Union.

Paper number 2000JD900503.

0148-0227/01/2000JD900503\$09.00

the treatments of aerosol-cloud interactions and aerosol and cloud radiative properties and evaluate the simulation of the direct and indirect radiative forcing, respectively, in MIRAGE.

To place this study in context, it is helpful to review some of the requirements of any estimate of the radiative forcing by anthropogenic aerosols, and the characteristics of the integrated models used in previous estimates of anthropogenic aerosol forcing.

One requirement of radiative forcing estimates is that the anthropogenic aerosol must be isolated from the natural aerosol. Although measurements can be used to estimate the radiative forcing by all aerosols in a column, it is much more difficult to distinguish the anthropogenic and natural components of the radiative forcing. Even if one could distinguish the natural and anthropogenic components of the aerosol, distinguishing the natural and anthropogenic forcing is confounded by the dependence of the anthropogenic forcing on the presence of the natural aerosol. This is particularly true for the so-called indirect radiative forcing by aerosols through their role as cloud condensation nuclei (CCN) because of the competition between aerosol particles for water as cloud droplets form; the activation of anthropogenic aerosol particles depends very much on the abundance of natural aerosol particles [Ghan *et al.*, 1998].

This suggests a second requirement: any estimate must treat all radiatively important (in terms of both direct and indirect radiative forcing) aerosol, natural as well as anthropogenic. In the case of indirect radiative forcing, all important components of the cloud condensation nuclei must be treated. As shown by Ghan *et al.* [1998], this includes components of the CCN that are important contributors to CCN surface area as well as number concentration. Thus sea-salt particles, although relatively few in number but often dominant in surface area, should be treated in models used to estimate the indirect radiative forcing.

A third requirement is that the influence of water uptake on the direct radiative forcing must be represented in a realistic manner. This includes treatment of the hysteresis in deliquescence.

A fourth requirement is that cloud-aerosol interactions be treated in a consistent manner. This includes not only the influence of the aerosol on cloud droplet number, droplet size, cloud liquid water content, cloud albedo, and cloud lifetime but also the influence of the cloud on the aerosol. Activated and unactivated aerosol should be distinguished when a cloud forms and should be recombined when the cloud dissipates. Aqueous-phase oxidation of sulfate in clouds, which is known to be an important aerosol production mechanism [Pham *et al.*, 1995; Feichter *et al.*, 1996], must be treated. Droplet collision-coalescence should reduce the aerosol number concentration as well as the droplet number concentration.

A fifth requirement is that the parameterizations of the key processes involving direct and indirect radiative forcing should be as physically based as possible. Although empirical parameterizations can be expedient, they are unlikely to be applicable to the full range of conditions encountered in the atmosphere. Physically based parameterizations are more capable of treating the diverse mixtures of aerosols found in the atmosphere.

MIRAGE was designed with the above requirements in mind and hence is a relatively complex model. Previous estimates of direct and indirect radiative forcing used

somewhat simpler models in order to develop understanding of the key processes that determine the forcing.

The earliest estimates of radiative forcing by anthropogenic aerosol were essentially back-of-the-envelope calculations [Bolin and Charlson, 1976; Charlson *et al.*, 1992]. Subsequent estimates (Table 1) used chemical transport models to determine the spatial distribution of the aerosol and either off-line radiative transfer codes or general circulation models to estimate the radiative forcing. The first estimate of the spatial distribution of the direct radiative forcing [Charlson *et al.*, 1991] used monthly mean column sulfate mass loadings, a single estimate of the aerosol radiative properties, and a very simple radiative transfer model. Subsequent estimates accounted for spatial variability in the relative humidity and its influence on the aerosol optical properties, first with monthly mean relative humidity [Kiehl and Briegleb, 1993] and then with hourly relative humidity [Boucher and Anderson, 1995; Haywood *et al.*, 1997; Chuang *et al.*, 1997; Haywood and Ramaswamy, 1998; Kiehl *et al.*, 2000]. The most recent estimates use on-line chemical transport models to calculate the aerosol mass concentration, specify the dry aerosol size distribution, use Köhler theory to determine water uptake, estimate the wet particle refractive index using volume mixing of the refractive indices of water and the dry particle, Mie theory to estimate the radiative properties for multiple wavelengths, and a delta-Eddington radiative transfer code to estimate the direct radiative forcing under cloudy as well as clear conditions. MIRAGE includes all of these features, and adds the prediction of aerosol number as well as mass for each of four lognormal modes. In addition, each mode can be composed of several internally mixed components (e.g., sulfate, methane sulfonic acid, organic carbon, black carbon, dust, and sea salt), using volume mixing to determine the refractive index of the composite aerosol.

Estimates of the indirect radiative forcing by anthropogenic aerosol have also become increasingly complex. Following the first back-of-the-envelope estimates, general circulation models have been used to estimate the forcing. The first GCM estimates [Jones *et al.*, 1994; Boucher and Lohmann, 1995; Jones and Slingo, 1996; Rotstayn, 1999] used monthly mean sulfate concentrations (simulated off-line by a chemical transport model) and empirical relationships between droplet number and either sulfate mass or aerosol number (determined from sulfate mass by assuming a prescribed size distribution). As an alternate to the use of a chemical transport model, Boucher [1995] used satellite estimates of droplet effective radius and inferred the anthropogenic forcing from the contrast between effective radius of the Southern and Northern Hemispheres. More recent estimates used on-line simulations of the atmospheric sulfur cycle. Feichter *et al.* [1997], Lohmann and Feichter [1997], and Kiehl *et al.* [2000] used an online sulfur cycle model that treated aqueous phase sulfur oxidation. Chuang *et al.* [1997] used a much simpler sulfur cycle model, but for the first time used a physically based parameterization of the relationship between droplet number and aerosol number. Of these studies, only Lohmann and Feichter [1997] accounted for the influence of droplet number on cloud liquid water. Rotstayn [1999] also treated the cloud liquid water feedback but used an off-line monthly mean sulfate concentration. The most recent estimate of the indirect forcing [Lohmann *et al.*, 2000] not only treated the influence of droplet number on cloud liquid water but also used a physically based prognostic treatment for droplet

Table 1. Characteristics of Previous Estimates of Direct Radiative Forcing

Reference	Aerosol Mass	Aerosol Composition	Relative Humidity	Water Uptake	Radiative Properties	Spectral Dependence
<i>Charlson et al.</i> [1991]	annual column	sulfate	constant, uniform	constant, uniform	constant	none
<i>Kiehl and Briegleb</i> [1993]	annual column	sulfate	monthly	empirical	Mie for dry aerosol	n, σ, ω, g
<i>Boucher and Anderson</i> [1995]	monthly	sulfate	hourly	laboratory measurements	Mie	n, σ, ω, g
<i>Haywood and Shine</i> [1995]	annual column	sulfate, soot	constant, uniform	constant, uniform	Mie	n, σ, ω, g
<i>Haywood et al.</i> [1997]	annual column	sulfate, soot	hourly	Kohler	Mie	n, σ, ω, g
<i>Tegen et al.</i> [1996]	monthly	soil dust		none	Mie	n, σ, ω, g
<i>Schult et al.</i> [1997]	monthly	sulfate, soot	80%	Kohler	Mie	n, σ, ω, g
<i>Haywood and Ramaswamy</i> [1998]	monthly	sulfate, soot	hourly	Kohler	Mie	n, σ, ω, g
<i>Myhre et al.</i> [1998]	monthly	sulfate, soot	monthly	Kohler	Mie	n, σ, ω, g
<i>Graf et al.</i> [1997]	monthly	sulfate	80%	constant	Mie	n, σ, ω, g
<i>Feichter et al.</i> [1997]	hourly	sulfate	80%	constant, uniform	constant, uniform	none
<i>Chuang et al.</i> [1997]	hourly	sulfate	hourly	Kohler	Mie	n, σ, ω, g
<i>van Dorland et al.</i> [1997]	monthly	sulfate	monthly	Kohler	Mie	n, σ, ω, g
<i>Penner et al.</i> [1998]	hourly	sulfate, soot, organic	hourly	Kohler	Mie	n, σ, ω, g
<i>Haywood et al.</i> [1999]	monthly	sulfate, soot, organic, dust, sea salt	80%	Kohler	Mie	n, σ, ω, g
<i>Grant et al.</i> [1999]	hourly	sulfate	hourly	Kohler	Mie	n, σ, ω, g
<i>Koch et al.</i> [1999]	hourly	sulfate	hourly	empirical	Mie	n, σ, ω, g
<i>Kiehl et al.</i> [2000]	hourly	sulfate	hourly	Kohler	Mie	n, σ, ω, g
<i>Tegen et al.</i> [2000]	hourly	sulfate, soot, organic, dust, seasalt	hourly	empirical	Mie	n, σ, ω, g

number that accounts for droplet sinks due to collision/coalescence and evaporation. The method for estimating indirect forcing in MIRAGE is very similar to that of *Lohmann et al.* [2000], but in MIRAGE, both the number and the mass of each aerosol mode change independently in response to the aerosol activation process.

This paper describes an estimate of the direct and indirect radiative forcing by anthropogenic sulfur. We focus on sulfur because its anthropogenic source is large and well known and because its microphysical properties (hygroscopicity, refractive index) are also well known. Most other estimates of direct and indirect forcing have also focused on anthropogenic sulfur. Although it might be argued that the use of empirical relationships between droplet number and sulfate concentration in other studies implicitly treats the effects of aerosol components that are correlated with sulfate, the distributions of the emissions of sulfur and other important aerosol (organic, sea salt, dust) are so different that it is unlikely that the empirical relationships treat the dependence of droplet number on anything but sulfate and perhaps industrial carbonaceous aerosol.

The present study is distinguished from previous estimates of both direct and indirect forcing by its prognostic treatment of aerosol number and by its treatment of multiple aerosol modes. The experiment design is described in section 2. Section 3 presents the estimate and the various components of the radiative forcing. A variety of sensitivity experiments are considered in section 4 to provide some evidence of the uncertainty of the estimate in the baseline experiment.

2. Experiment Design

Radiative forcing by aerosols is usually separated into two components. One, called direct radiative forcing, accounts for the direct interaction of the particles with radiation, through scattering, absorption, and emission. The second component, called indirect radiative forcing, accounts for the influence of the particles on cloud droplet number concentration and hence cloud liquid water, cloud albedo, and cloud lifetime (aerosols may also affect ice clouds through their role as ice nuclei, but this influence has not yet been addressed in MIRAGE because of the difficulty of relating ice nuclei to aerosol concentra-

tions and physical properties). These two components of radiative forcing are often associated with the clear sky and cloudy sky, respectively, because direct forcing is obscured by clouds for a cloudy sky and because indirect forcing requires clouds. However, aerosol particles are still present beneath, above, and to a lesser extent within clouds, so direct interaction of aerosol particles with radiation still occurs for cloudy skies and can be important for aerosols above clouds or beneath optically thin clouds. Estimates of direct forcing that neglect the contribution from the cloudy sky will underestimate the direct forcing, while estimates that neglect the obscuration by clouds will overestimate the direct forcing. We have therefore designed our experiments to estimate direct and indirect radiative forcing for both cloudy and clear skies. We do so by adding an additional radiation calculation in each simulation: the radiative flux at the top of the atmosphere (F) is calculated both with the aerosols treated in the simulation (F_{aer}) and without any aerosols (F_{noaer}). The direct radiative impact of aerosols in a simulation (F_{direct}) can then be determined from the difference between F_{aer} and F_{noaer} .

To estimate the direct and indirect forcing by anthropogenic sulfate aerosol, we perform two simulations, one with anthropogenic sulfur emissions and one without. The direct radiative forcing due to the anthropogenic sulfate aerosol is then

$$\Delta F_{\text{direct}} = \Delta F_{\text{aer}} - \Delta F_{\text{noaer}}, \quad (1)$$

where Δ denotes the difference between the simulations with and without the anthropogenic sulfate aerosol. Note that ΔF_{direct} includes the contribution of the cloudy sky to the direct forcing. The indirect forcing due to anthropogenic sulfate aerosol is then the difference between the total forcing by the anthropogenic sulfate aerosol ($\Delta F = \Delta F_{\text{aer}}$) and its direct forcing,

$$\Delta F_{\text{indirect}} = \Delta F - \Delta F_{\text{direct}} = \Delta F_{\text{aer}} - \Delta F_{\text{direct}} = \Delta F_{\text{noaer}} \quad (2)$$

Note that according to the last equality the indirect forcing is independent of the radiative properties of the aerosol and depends only on the influence of the aerosol on the cloud droplet number, cloud liquid water, cloud albedo, cloud lifetime, and cloud area.

Note also that the state of the atmosphere is not the same in the simulations with and without anthropogenic sulfate aerosol. Although this is inconsistent with the definition of forcing as being an external force imposed upon the climate system, it is not possible to account for the influence of droplet number on cloud liquid water (an important component of the indirect forcing) without allowing the cloud liquid water to differ between simulations. However, by prescribing the ocean surface conditions and focusing on the shortwave forcing, we do not expect the response of the atmosphere and land surface to confound the estimate of the radiative forcing. Indeed, in the experiments described here the longwave radiation balance at the top of the atmosphere is insensitive to the presence of the aerosol, indicating that the response of temperature to the aerosol is weak.

To provide additional information about indirect radiative forcing, we have added to each simulation a second calculation of the clean-sky radiative flux at the top of the atmosphere, F_N , in which the droplet number mixing ratio used to determine the cloud radiative properties is prescribed at 10^8 kg^{-1} . If the cloud optical depth τ is expressed [Twomey, 1991],

$$\tau = \frac{4\pi h}{3} \left(\frac{w}{\rho_w} \right)^{2/3} N^{1/3}, \quad (3)$$

where h is the cloud thickness, w is the cloud liquid water content, N is the droplet number concentration, and ρ_w is the density of liquid water, then differences in cloud optical depth between simulations with and without anthropogenic sulfate aerosol,

$$\frac{\Delta\tau}{\tau} \approx \frac{2\Delta w}{3w} + \frac{\Delta h}{h} + \frac{\Delta N}{3N}, \quad (4)$$

can only arise from differences in the liquid water content, cloud thickness, and number concentration of droplets. Given the definition of F_N , the difference in F_N between the two simulations must reflect changes in the liquid water content and cloud thickness. Since we expect that over a period of months or years ΔF_N will be dominated by changes in liquid water content (which should increase with increasing droplet number) rather than changes in cloud thickness, we shall refer to ΔF_N as the indirect forcing due to the cloud liquid water feedback. The indirect forcing can then be decomposed into

$$\Delta F_{\text{indirect}} = \Delta F_N + \Delta F_w. \quad (5)$$

The last term (determined as a residual) largely accounts for radiative forcing due to changes in droplet effective radius associated with changes in droplet number rather than liquid water content, although such an association is only approximate. This can be seen by expressing the cloud optical depth

$$\tau = \frac{3wh}{2r\rho_w}. \quad (6)$$

If the liquid water content and cloud thickness do not change, then changes in optical depth are due to changes in droplet size r . We therefore refer to the second term in (5) as the indirect forcing due to changes in droplet size, even though droplet size can also change as liquid water content changes.

Note that nowhere in the above discussion is cloud fraction mentioned. One could decompose ΔF_N into components associated with change in liquid water content and cloud fraction, but such a decomposition would require an arbitrary selection of a nominal liquid water content. We shall find that the cloud fraction changes little in response to anthropogenic sulfate, so such a decomposition would yield little additional information.

Although anthropogenic aerosol arises from emissions of primary carbonaceous and soil dust particles and of gaseous precursors of secondary carbonaceous, sulfate and nitrate aerosol, our focus in this study is on anthropogenic sulfate aerosol. Our baseline experiment therefore consists of two simulations, one with and one without anthropogenic sulfur emissions. The two simulations are identical in all other respects, including primary and secondary carbonaceous aerosol, natural sulfur aerosol, soil dust, and sea-salt. See E2000 for a description of the aerosols and aerosol precursors treated in MIRAGE.

The period of the experiment is June 1994 to May 1995, after spinning up the aerosol and oxidants beginning in March 1994 and the carbon monoxide for a full year. Given the dominance of pollutant emissions from the Northern Hemisphere, 1 year is the minimum simulation duration required to estimate the radiative forcing. Nudging toward

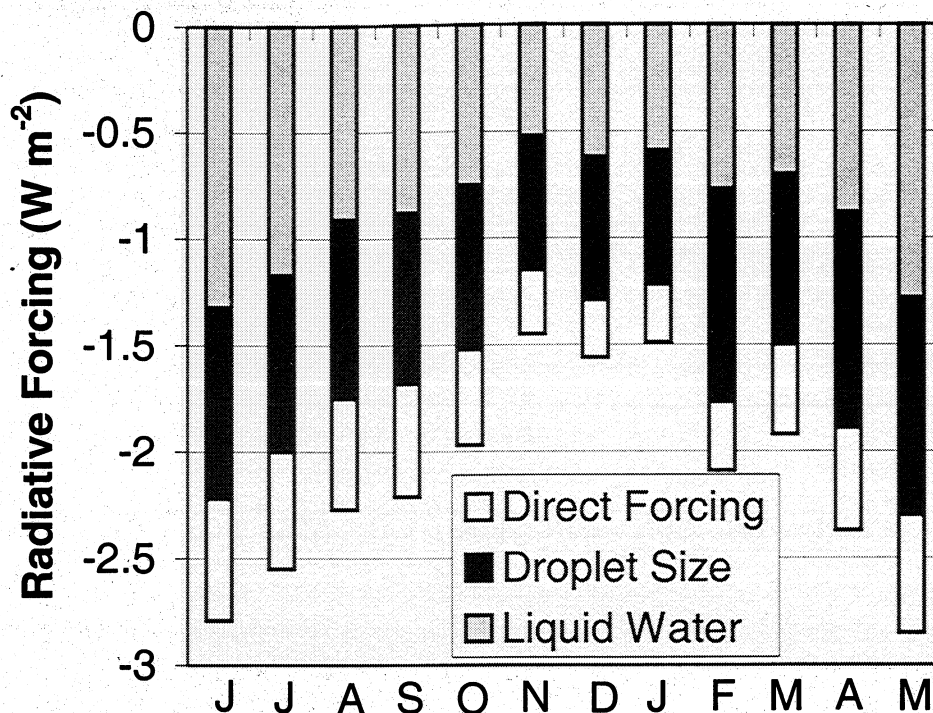


Figure 1. Global and monthly mean anthropogenic sulfate radiative forcing due to direct scattering, decreased droplet size, and increased liquid water content, as simulated by MIRAGE for the baseline experiment.

the European Centre for Medium-Range Weather Forecasts (ECMWF) analyzed winds and temperature is applied to reduce the sensitivity of the simulated winds (and the production of sea-salt and dust particles). Sampling error associated with natural variability of the atmosphere is estimated from the variability of the monthly means, accounting for the predictable variations due to the seasonal cycle of insolation.

3. Baseline Results

In the baseline experiment, MIRAGE is run at T42 spectral (2.8° latitude and longitude) resolution with the physics and chemistry described by E2000. We begin our discussion with the global and annual mean forcing, then progress to seasonal and zonal mean forcing, and then to the various components of the forcing.

The global and annual mean direct and indirect radiative forcing are -0.44 ± 0.05 and -1.7 ± 0.1 W m^{-2} , respectively, where the uncertainty here only includes the month-to-month variability of the forcing after the first harmonic of the seasonal cycle of the forcing is removed. Figure 1 shows the seasonal cycle of the forcing, with the indirect forcing separated into its contributions from changes in liquid water content and droplet size. All components of the forcing are weaker during the months November to January, when less sunlight is available in the more polluted Northern Hemisphere. In each month, about half of the indirect forcing is due to the cloud liquid water feedback.

Some estimates of the indirect forcing use the change in the shortwave cloud radiative forcing. Although this is reasonable if the direct forcing by aerosols is neglected, such a treatment can introduce larger errors in the estimate of

indirect forcing if direct forcing is also calculated. In the baseline experiment the change in the shortwave cloud radiative forcing is -1.3 W m^{-2} , much smaller than $\Delta F_{\text{indirect}} = -1.7$ W m^{-2} .

The zonal mean distribution of the annual mean direct forcing is illustrated in Figure 2. As might be expected, most of the direct forcing is near the regions with the strongest anthropogenic sulfur emissions, in the midlatitudes of the Northern Hemisphere.

The distribution of the direct forcing is quite different from the distribution of the anthropogenic sulfate. Figure 3 illustrates the zonal mean distribution of the annual mean aerosol optical depth for the baseline simulations with and without anthropogenic sulfur. The largest increase in aerosol optical depth due to anthropogenic sulfur is in the Arctic, but because most of the increase occurs during the Arctic winter, the direct forcing in the Arctic is quite weak. The large optical depth in the midlatitudes of the Southern Hemisphere is associated with water uptake on sea-salt particles [Ghan *et al.*, this issue (a)]. Most of the direct forcing by anthropogenic sulfur is due not to the increased sulfate loading in the atmosphere but to the increased aerosol water loading (Figure 4).

The global mean direct forcing is comparable to estimates by other investigators, even though the global mean anthropogenic sulfate burden (4.0 mg m^{-2}) is significantly larger than in other studies. The direct forcing normalized by the sulfate burden is -110 W g^{-1} , smaller than in any other study [Myhre *et al.*, 1998]. The weakness of the normalized forcing is due to several factors. First, the ECMWF-analyzed relative humidity (which approaches 100% far less frequently than the relative humidity simulated by MIRAGE [Ghan *et al.*, this issue (a)]) is used to calculate water uptake in MIRAGE.

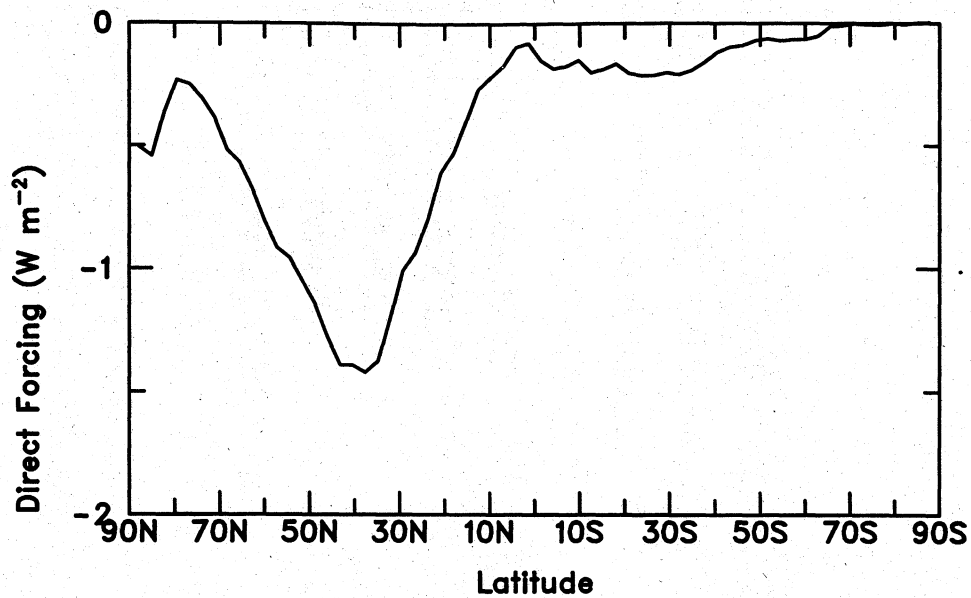


Figure 2. Zonal and annual mean direct radiative forcing due to anthropogenic sulfate, as simulated by MIRAGE for the baseline experiment.

Second, particles in MIRAGE can be either wet or dry for relative humidity between the crystallization and the deliquescence points [Ghan *et al.*, this issue (a)], whereas other models treat only wet particles and hence overestimate the radiative forcing for some particles. Third, in MIRAGE a larger fraction of the anthropogenic sulfate burden is simulated for the Arctic winter (where little insolation is available to produce a radiative forcing) than in models that do not couple sulfate with cloud microphysics [Pham *et al.*, 1996; Feichter *et al.*, 1996; Chin and Jacob, 1996]; models that, like MIRAGE, couple sulfate with cloud microphysics [Lohmann *et al.*, 2000] also simulate large sulfate loadings in the Arctic winter. Fourth, MIRAGE predicts the number as well as mass

of each aerosol mode, so accumulation mode particles can be smaller and hence less radiatively active than in other models that prescribe the aerosol size distribution. Fifth, the direct radiative forcing by particles that have been activated to form cloud droplets is neglected in MIRAGE but not in other studies [Ghan and Easter, 1998]. Sixth, because MIRAGE assumes sulfate particles are internally mixed with black carbon, the addition of sulfate on particles with black carbon can increase the absorption by black carbon and hence reduce the scattering by sulfate. These causes for the weaker normalized direct forcing are explored in a series of sensitivity experiments discussed in section 4.

The zonal mean distribution of the annual mean indirect

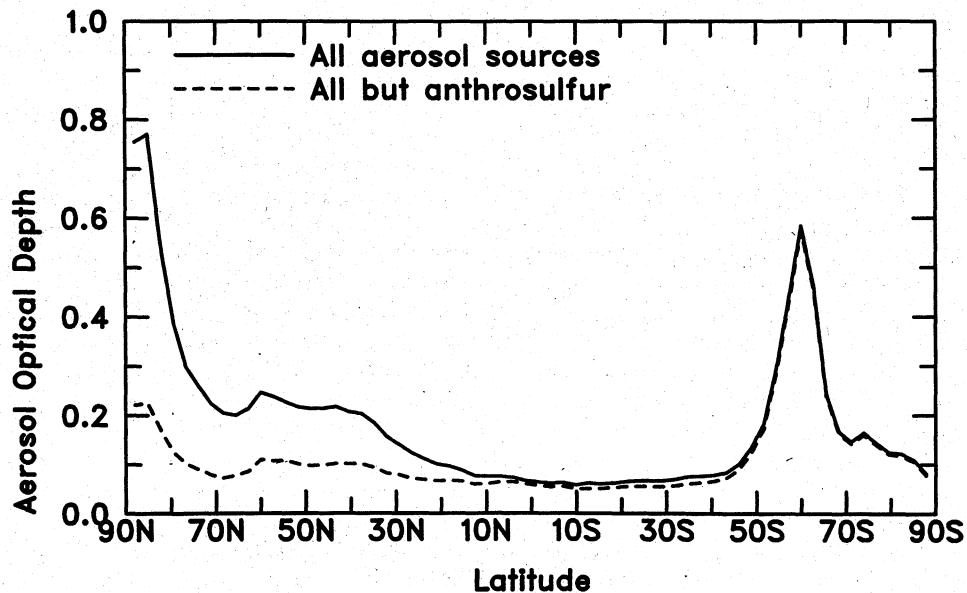


Figure 3. Zonal and annual mean aerosol optical depth for the baseline simulations with and without anthropogenic sulfur.

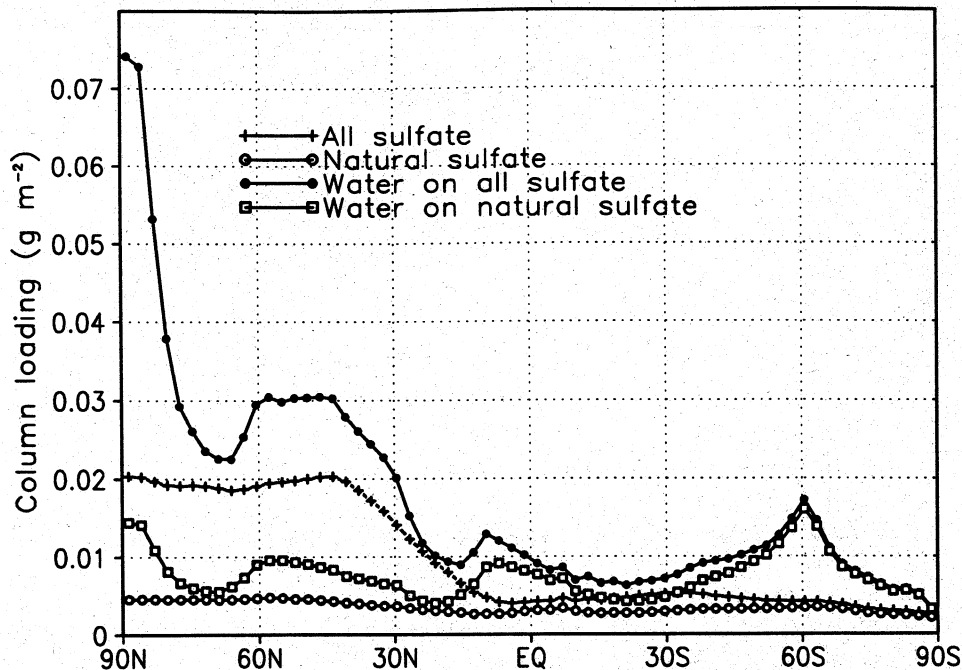


Figure 4. Annual and zonal mean column loading of accumulation mode sulfate and liquid water for the simulations with and without anthropogenic sulfur emissions.

forcing is illustrated in Figure 5. The distribution is rather noisy because of the variability in clouds between the two simulations, but the forcing is clearly strongest in the midlatitudes of the Northern Hemisphere. However, the fractional contribution of the Southern Hemisphere to the total indirect forcing (19%) is somewhat larger than for direct forcing (16%), which can be explained by cloud albedos in the cleaner Southern Hemisphere being more susceptible to increases in aerosol [Twomey, 1991].

The indirect forcing is, of course, driven by changes in the droplet number. Figure 6 shows the zonal mean distribution of the annual mean column droplet number for the baseline

simulations with and without anthropogenic sulfur. The column droplet number is nearly doubled by the anthropogenic sulfur in most of the Northern Hemisphere, with increases of only 20% in the Southern Hemisphere as far south as 45°S. In the global mean the column droplet number increases from $2.55 \times 10^6 \text{ cm}^{-2}$ without to $3.47 \times 10^6 \text{ cm}^{-2}$ with anthropogenic sulfur.

As might be expected, the cloud droplet effective radius is reduced by anthropogenic sulfur. The zonal, annual, and vertical mean (weighted by cloud water) droplet radius in the simulation with anthropogenic sulfur (Figure 7) is reduced by about 10% in most of the Northern Hemisphere and by a few

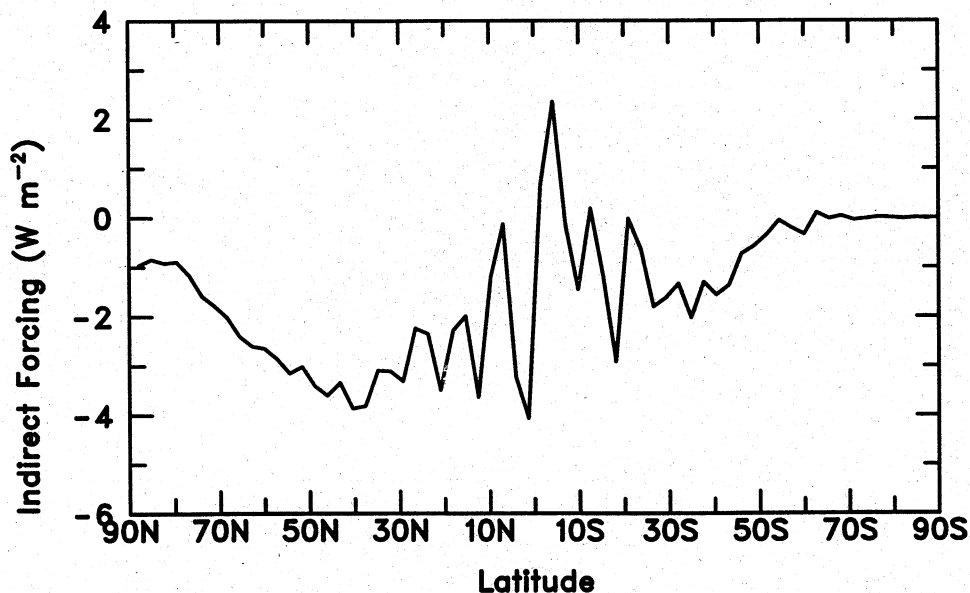


Figure 5. Zonal and annual mean indirect forcing due to anthropogenic sulfur, as simulated by MIRAGE for the baseline experiment.

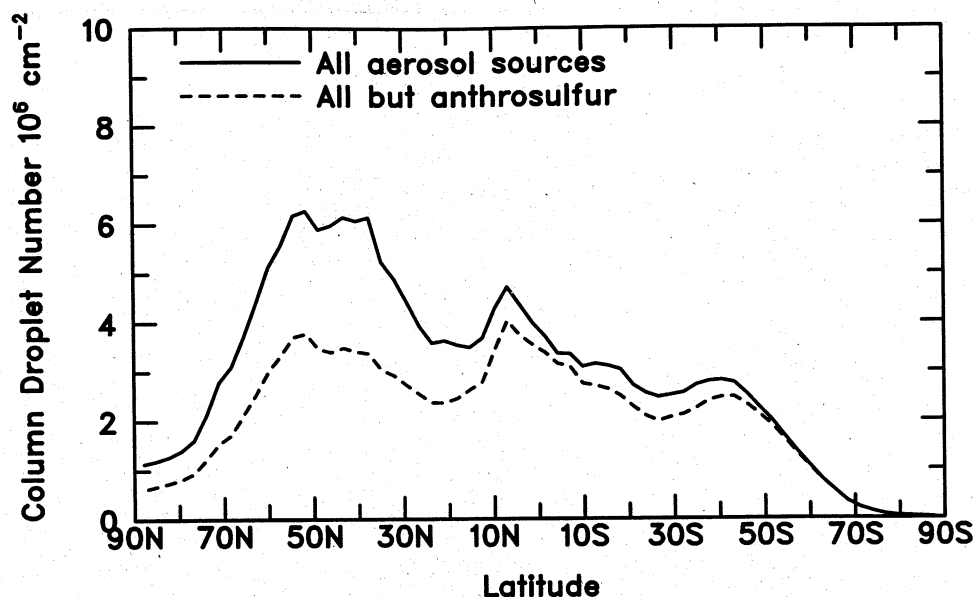


Figure 6. Zonal and annual mean column droplet number (10^6 cm^{-2}) simulated in the baseline experiment with and without anthropogenic sulfur.

percent in the Southern Hemisphere, with a global mean reduction of 4.3%. Even in the simulation without anthropogenic sulfur the droplet radius is larger in the Southern Hemisphere than in the Northern Hemisphere, reflecting the larger emissions of organic and black carbon and soil dust in the Northern Hemisphere.

As demonstrated by Lohmann and Feichter [1997] and Rotstayn [1999], the cloud liquid water content responds to changes in droplet number through the influence of droplet number on the autoconversion of cloud water to rain. Figure 8 shows the zonal and annual mean column cloud water in each MIRAGE simulation. Anthropogenic sulfur increases the column cloud water by about 10% in much of the

Northern Hemisphere but little elsewhere. The global mean column cloud water increases from 54.4 to 56.3 g m^{-2} , a 3.5% increase. Such an increase is smaller than the 6% increase estimated by Rotstayn [1999] and Lohmann *et al.* [2000] for anthropogenic sulfur and much smaller than the 17-32% increase estimated by Lohmann and Feichter [1997].

Albrecht [1989] suggested that cloud fraction might be sensitive to aerosol loading. Lohmann and Feichter [1997] estimate a 1-3% increase in cloud fraction due to anthropogenic sulfur. Rotstayn [1999] estimates a 1% increase. Lohmann *et al.* [2000], on the other hand, estimate an increase of only 0.1%, and MIRAGE simulates an increase of only 0.2%.

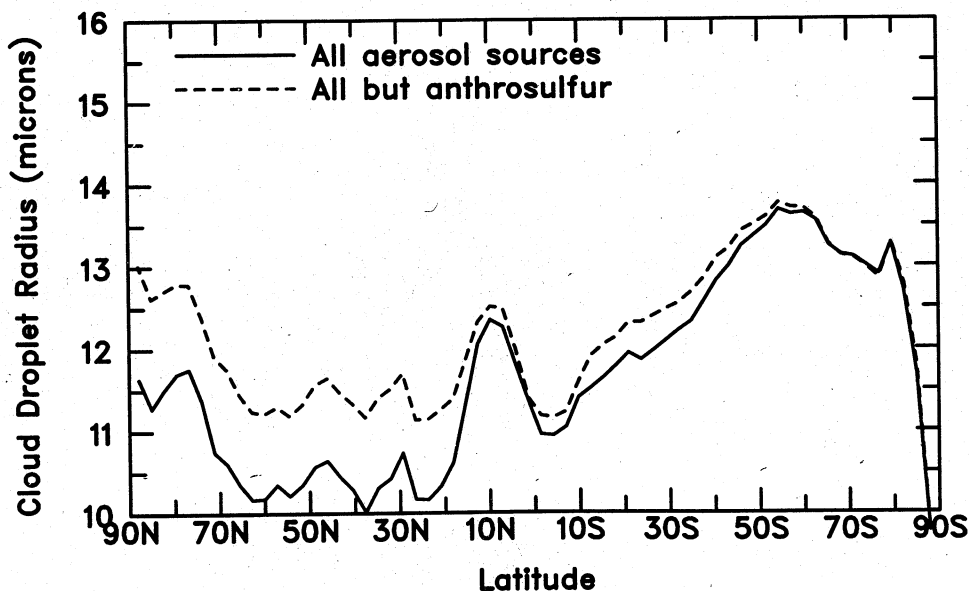


Figure 7. Zonal, annual, and vertical mean (weighted by cloud water) droplet effective radius simulated with and without anthropogenic sulfur.

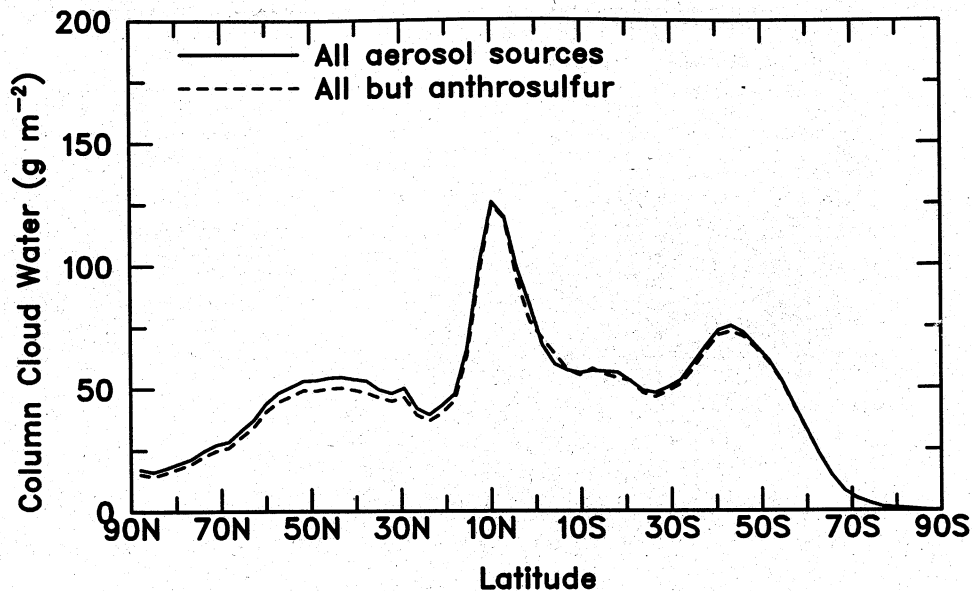


Figure 8. Zonal and annual mean column cloud water simulated with and without anthropogenic sulfur.

Given the relatively small changes in the droplet effective radius and column liquid water, the magnitude of the indirect forcing simulated by MIRAGE is larger than might be expected on the basis of experiments by other investigators. Lohmann and Feichter's [1997] baseline estimate of global mean indirect forcing (-1.4 W m^{-2}) is smaller than the MIRAGE estimate (-1.7 W m^{-2}), yet their global mean column cloud water increases much more than in the MIRAGE simulation. Lohmann et al.'s [2000] baseline estimate of the indirect forcing due to anthropogenic sulfur (-0.4 W m^{-2}) is much smaller than the MIRAGE estimate, but their column cloud water increases by more than in MIRAGE. The much smaller estimate of indirect forcing by Lohmann et al. [2000] can be partially explained by the fact that Lohmann et al. place a lower bound of 40 cm^{-3} on the droplet number concentration, while MIRAGE does not; however, the larger increase in column cloud water in the Lohmann et al. experiment should produce an indirect forcing at least as large as in the MIRAGE experiment. Rotstayn's [1999] indirect forcing estimate (-2.1 W m^{-2}) is somewhat larger than the MIRAGE baseline, but the changes in effective radius and column cloud water are about twice as large as in MIRAGE. These apparent inconsistencies suggest that variations in space and time need to be considered to fully reconcile differences between estimates by different models.

The differences between the droplet number concentration in the MIRAGE simulations with and without anthropogenic sulfur are, of course, driven by differences in the aerosol. To illustrate this influence, Figure 9 shows the zonal and annual mean CCN concentration at a supersaturation of 0.1% for both simulations. Although such a supersaturation is not necessarily representative of the maximum supersaturation achieved in all clouds, it is a typical value. The CCN concentration at $S=0.1\%$ provides an integrated measure of the influence of all four simulated aerosol modes on cloud droplet number, provided updraft velocities are sufficient to produce supersaturations of 0.1%. According to Figure 9 the CCN concentrations are generally greatest near the surface, except

over the Arctic Ocean, where an elevated plume of aerosol is evident in both simulations. CCN concentrations are doubled by anthropogenic sulfur throughout most of the lower troposphere in the Northern Hemisphere and tripled below 700 hPa northward of 20°N. These changes are much larger than the proportional changes in droplet number illustrated in Figure 6, reflecting the sublinear dependence of droplet number on CCN concentration.

4. Sensitivity Experiments

Natural variability is only one source of uncertainty in estimates of direct and indirect radiative forcing. Here we show that the treatment of a variety of different processes produces greater uncertainty than that due to natural variability. We use MIRAGE to estimate the sensitivity of the radiative forcing to (1) horizontal resolution, (2) the treatment of cloud droplet number, (3) the treatment of cloud microphysics, (4) the treatment of aerosol size distribution, and (5) the treatment of relative humidity. The global mean forcing for each sensitivity experiment is summarized in Table 2.

4.1. Sensitivity to Horizontal Resolution

In the baseline experiment the horizontal resolution is T42 spectral (2.8° latitude and longitude). To determine the sensitivity to horizontal resolution, we repeated the experiment at R15 spectral (4.5° latitude by 7.5° longitude) resolution. Nudging toward the ECMWF-analyzed winds and temperature is retained to reduce the sensitivity of the simulated winds to resolution.

The global mean direct and indirect shortwave radiative forcing by anthropogenic sulfate both change significantly. The direct radiative forcing weakens from -0.44 to -0.34 W m^{-2} , while the indirect forcing strengthens from -1.7 to -2.4 W m^{-2} .

The weakening of the direct forcing can be attributed to both a smaller increase in sulfate loading and a smaller

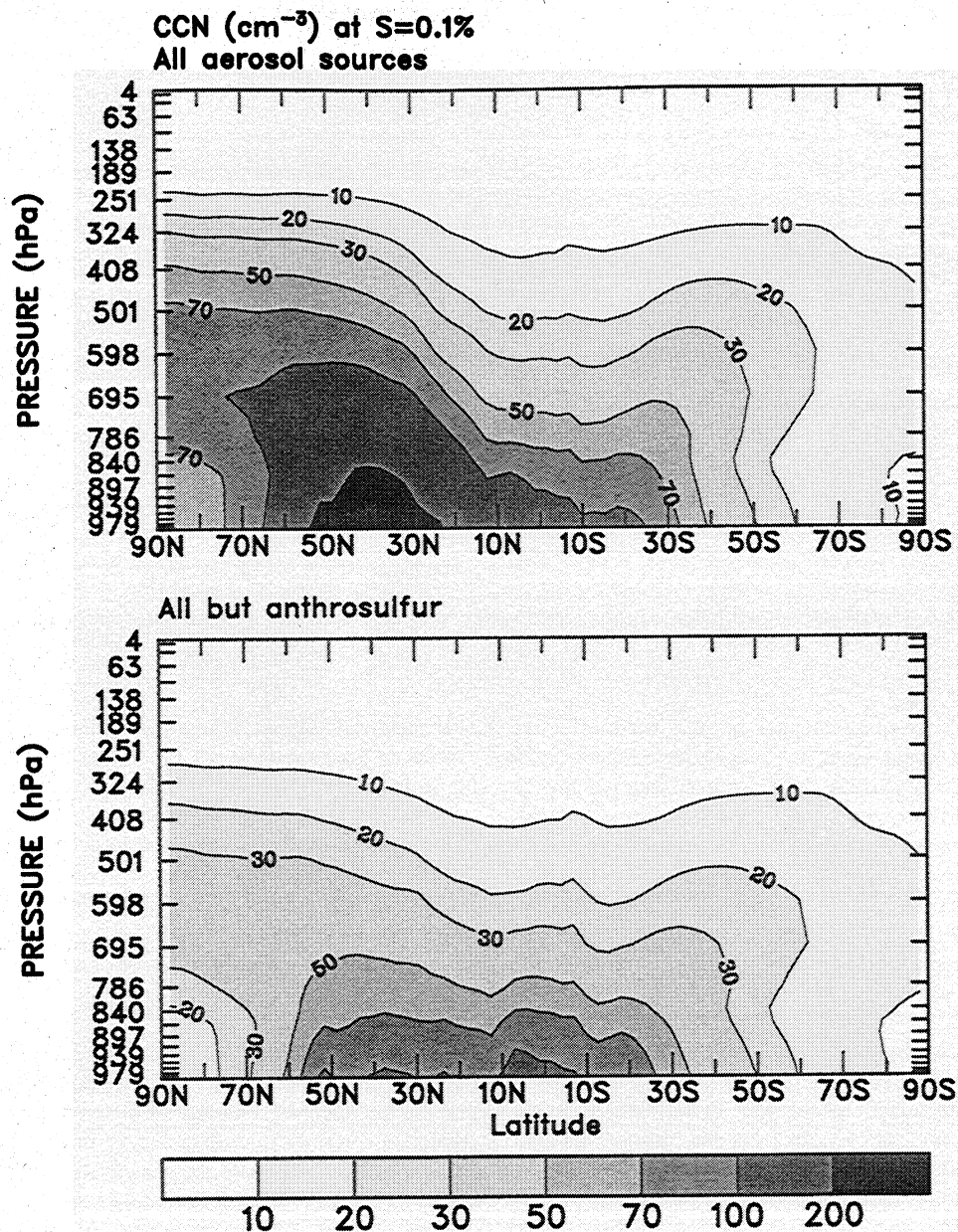


Figure 9. Zonal and annual mean CCN concentration (cm^{-3}) at a supersaturation of 0.1% simulated with (above) and without (below) anthropogenic sulfur.

increase in aerosol water loading. Table 3 summarizes the annual and global means of column droplet number, column liquid water, mean droplet radius, cloud optical depth, column accumulation mode sulfate loading, and column accumulation mode aerosol water for the simulations with and without anthropogenic sulfate. The column sulfate increases by 5.5 mg m^{-2} at T42 resolution but by only 4.7 mg m^{-2} at R15 resolution, while the column aerosol water increases by 7.3 mg m^{-2} at T42 resolution and by 6.6 mg m^{-2} at R15 resolution. Since the ratio of aerosol water to sulfate is about the same at both T42 and R15 resolution, it is probable that the smaller anthropogenic aerosol water loading at R15 resolution is due to the smaller anthropogenic sulfate loading. The lower sulfate loadings at R15 resolution are due to changes in clouds and precipitation, which strongly affect the sulfur cycle.

The stronger indirect forcing at R15 resolution is due to larger forcing due to changes in both droplet size and column cloud water. The forcing due to changes in droplet size increases from -0.8 W m^{-2} at T42 resolution to -1.1 W m^{-2} at R15 resolution, while the forcing due to increased liquid water path increases from -0.9 to -1.4 W m^{-2} . This greater sensitivity is driven by larger changes in droplet number at R15 resolution (Table 2), which are predicted in spite of smaller increases in sulfate loading. The ratio of column droplet number for the simulations with and without anthropogenic sulfur is similar for R15 and T42 resolution, but the difference is larger at R15 resolution because the column droplet number is larger at R15 resolution for both simulations. It is not all clear why the column droplet number is larger at R15 resolution than at T42 resolution, especially when the column sulfate and column CCN concentrations are

Table 2. Global Annual Mean Top-of-the-Atmosphere Radiative Forcing (W m^{-2}) for Baseline and Sensitivity Simulations

	T42	R15	Diagn N_d	Autoconv	Diagn N_a	Sim RH
Droplet size	-0.8	-1.1	-0.7	-1.4	-1.4	-1.1
Liquid water	-0.9	-1.4	-0.9	-1.8	-1.7	-1.6
Indirect shortwave	-1.7	-2.4	-1.6	-3.2	-3.1	-2.7
Direct shortwave	-0.44	-0.34	-0.35	-0.35	-0.35	-0.54
Total shortwave	-2.1	-2.8	-2.0	-3.5	-3.4	-3.2
Total longwave	0.08	0.18	0.14	0.19	0.19	0.15

"T42" and "R15" are simulations with baseline model physics at T42 and R15 spectral resolution. Diagn N_d , Autoconv, Diagn N_a , and Sim RH are simulations with diagnosed cloud droplet number, Tripoli and Cotton [1980] autoconversion, diagnosed aerosol number, and aerosol water uptake calculated with CCM2-simulated relative humidity, respectively (all at R15 resolution).

smaller at R15 resolution. The explanation must lie in the droplet number budget.

The longwave forcing by anthropogenic sulfate also increases substantially, from 0.08 W m^{-2} at R15 resolution to 0.18 W m^{-2} at T42 resolution. About half of the longwave forcing is from the clear sky and half from the cloud forcing. Since we expect a much smaller direct forcing by the predominantly accumulation mode sulfate particles, most of the clear-sky forcing is likely to be due to surface cooling and hence is not a measure of the external longwave forcing by anthropogenic sulfate. The change in the cloud forcing is associated with changes in cloud water content.

4.2. Predicted Versus Diagnosed Droplet Number

MIRAGE has an option to either predict droplet number from the droplet conservation equation [Ghan *et al.*, 1997b] or diagnose the droplet number from the number nucleated. The latter treatment neglects droplet loss due to mixing/evaporation, collision/coalescence, and collection by precipitation. To determine the sensitivity of the radiative forcing to

the treatment of these processes, we have run MIRAGE at R15 resolution with diagnosed droplet number.

One might expect simulated droplet numbers to be greater with diagnosed droplets because droplet sinks are neglected. In fact, MIRAGE predicts the opposite response, with only about one third as many droplets simulated with diagnosed droplet number compared with predicted number (Table 3). How can this be? The explanation begins with the fact that the droplet nucleation depends on updraft velocity. MIRAGE calculates droplet nucleation for a spectrum of updrafts, integrating over a Gaussian distribution of updraft velocity. For predicted droplet number, MIRAGE calculates the flux of droplets into the base of old clouds, integrated over the distribution of updraft velocity. The calculation of the flux weights the droplet nucleation by the updraft velocity. Since the droplet nucleation increases with updraft velocity, the flux emphasizes the higher nucleation associated with the stronger updrafts. For diagnosed droplet number, MIRAGE simply integrates the number nucleated over the distribution of vertical velocity. This produces a lower droplet number because

Table 3. Global Annual Means of Column Droplet Number (N_d), Column Liquid Water (LWP), Droplet Effective Radius (r_{eff}), Cloud Optical Depth (τ_{cld}), Accumulation Mode Column Ammonium Sulfate (SO_4), Accumulation Mode Column Aerosol Water (aerwtr), and Aerosol Optical Depth (τ_{aer}) for Baseline and Sensitivity Simulations

	T42	R15	Diagn N_d	Autoconv	Diagn N_a	Sim RH
N_d (A) 10^6 cm^{-2}	3.47	4.65	1.53	4.25	3.70	4.90
N_d (N)	2.55	3.32	1.16	2.81	2.39	3.43
N_d (Δ)	0.92	1.33	0.36	1.44	1.31	1.47
LWP (A) g m^{-2}	56.3	63.1	56.5	41.8	58.7	63.9
LWP (N)	54.4	59.8	54.1	36.6	54.7	60.4
LWP (Δ)	1.9	3.3	2.4	5.2	4.1	3.5
r_{eff} (A) μm	11.62	11.13	13.06	10.19	11.68	11.04
r_{eff} (N)	12.14	11.76	13.70	10.99	12.51	11.71
r_{eff} (Δ)	-0.52	-0.64	-0.64	-0.80	-0.83	-0.67
τ_{cld} (A)	9.1	10.4	8.0	7.6	9.3	10.6
τ_{cld} (N)	8.5	9.4	7.4	6.3	8.2	9.5
τ_{cld} (Δ)	0.6	1.0	0.7	1.3	1.1	1.1
SO_4 (A) mg m^{-2}	8.8	7.8	6.9	7.7	7.8	8.4
SO_4 (N)	3.3	3.1	2.8	3.0	3.1	3.3
SO_4 (Δ)	5.5	4.7	4.1	4.6	4.7	5.1
aerwtr (A) mg m^{-2}	15.4	15.9	14.7	16.0	12.8	50.5
aerwtr (N)	7.4	7.4	6.5	7.4	6.0	22.7
aerwtr (Δ)	8.0	8.5	8.2	8.6	6.8	27.8
τ_{aer} (A)	0.139	0.141	0.127	0.140	0.130	0.499
τ_{aer} (N)	0.097	0.102	0.092	0.100	0.092	0.380
τ_{aer} (Δ)	0.042	0.039	0.035	0.040	0.038	0.119

The A is from simulation with all sources, N is from simulation with all sources but anthropogenic sulfur, and Δ is the difference between them.

the vertical velocity spectrum includes both updrafts and downdrafts, and no droplets are nucleated in downdrafts, and the integration over the updrafts does not emphasize the stronger updrafts. Thus the difference is largely an artifact of the treatment of droplet nucleation.

Another factor contributing to the lower droplet numbers with diagnosed droplets is the feedback of droplet number on aerosol number [Baker and Charlson, 1990]. If droplet numbers are lower with diagnosed droplets then autoconversion is stronger, which depletes aerosol number by collision/coalescence and precipitation. The accumulation mode aerosol number concentrations are in fact about 40% lower with diagnosed droplet number compared with predicted droplet number.

The direct forcing does not change, but the indirect forcing with diagnosed droplet number is only -1.6 W m^{-2} in the global and annual mean, much smaller than for predicted droplet number at R15 resolution (-2.4 W m^{-2}). The reduction in the forcing is due to smaller changes in both column liquid water and droplet size, which are due to the smaller change in droplet number (both in terms of the absolute difference and the difference normalized by the simulation with all sources). The smaller response of droplet number to anthropogenic sulfur when droplet number is diagnosed may be due to greater competition between particles for water at the lower updraft velocities that are weighted more when droplets are diagnosed than when predicted from the integral of the flux of nucleated droplets into the cloud.

4.3. Sensitivity to the Parameterization of Autoconversion

Autoconversion is the process in which droplets collide with each other and coalesce to form larger droplets and precipitation. The baseline simulation uses the Ziegler [1985] parameterization of autoconversion, which treats the influence of autoconversion on both droplet number and cloud liquid water content. To test the sensitivity of the radiative forcing to the treatment of autoconversion, we have replaced the Ziegler parameterization with the Tripoli and Cotton [1980] parameterization and repeated the R15 simulations with and without anthropogenic sulfur. Although the Tripoli and Cotton parameterization does not treat the influence of autoconversion on droplet number, we can relate the influence of autoconversion on cloud water content to its influence on droplet number by assuming autoconversion does not change the shape of the droplet size distribution, and we apply the first-order loss rate of cloud liquid water by autoconversion ($1/q\partial q/\partial t$) to droplet number also. Note that such a treatment only accounts for the influence of autoconversion on droplet number when droplets are large enough for significant coalescence to begin.

The direct forcing does not change, but the indirect forcing due to anthropogenic sulfur is significantly stronger using the Tripoli and Cotton [1980] parameterization. The global mean indirect forcing is -3.2 W m^{-2} , much stronger than the -2.4 W m^{-2} forcing with the Ziegler [1985] parameterization. Both the column cloud water and the droplet size contribute to the stronger forcing. The largest factor is the increase in column cloud water, which in the global and annual mean is 3.3 g m^{-2} with the Ziegler [1985] parameterization and 5.2 g m^{-2} with the Tripoli and Cotton [1980] parameterization. The cloud water sink from autoconversion is much weaker using the Tripoli and Cotton [1980] parameterization.

4.4. Predicted Versus Diagnosed Aerosol Number

In the baseline version of MIRAGE, aerosol number concentration is predicted independently of aerosol mass concentration, permitting the aerosol size distribution to change in response to different processes. All other global aerosol models prescribe the shape of the aerosol size distribution and diagnose the aerosol number concentration from the aerosol mass concentration. To determine the sensitivity of the radiative forcing to the treatment of aerosol number, we have repeated the R15 simulation with aerosol number diagnosed rather than predicted. The number model radii and geometric standard deviations of each of the four aerosol modes are listed in Table 4. For the Aitken and accumulation modes the values represent a synthesis of tropospheric aerosol observations from the literature. The values for the coarse sea-salt mode are from O'Dowd *et al.* [1997] and are used for coarse sea-salt emissions. The values for the coarse dust mode are derived from the observed mass size distribution of east Asian dust by Arao and Ishizaka [1986].

The direct forcing does not change, but the indirect forcing increases in strength from -2.4 W m^{-2} with predicted aerosol number to -3.1 W m^{-2} with diagnosed aerosol number. This increase in the strength of the indirect forcing can be traced to the increase in the accumulation mode number concentration. Figure 10 compares the column number concentration of the accumulation mode for the R15 experiments with predicted and diagnosed aerosol number. For the simulations without anthropogenic sulfur the simulated aerosol number is much larger when aerosol number is predicted rather than diagnosed, because the treatment of nucleation scavenging (which preferentially removes particles larger than roughly $0.1 \mu\text{m}$ diameter) is much more realistic with predicted number. When aerosol number is diagnosed, the number fraction activated is assumed to be the same as, rather than smaller than, the mass fraction activated. Droplet number concentrations are significantly larger when aerosol number is predicted rather than diagnosed.

When anthropogenic sulfate is added to the simulations, the simulation with predicted aerosol number has a much smaller response to the added pollutant because sulfate is primarily a secondary aerosol and hence adds relatively more mass rather than number to the accumulation mode aerosol. Thus the impact of anthropogenic sulfate formation on accumulation mode number is unrealistically large when aerosol number is diagnosed. This produces a significantly larger increase in CCN concentration (less so than the increase in aerosol number because CCN concentration depends on size as well as number), which in turn produces larger increases in droplet number concentrations, more liquid water (because of slower autoconversion), and stronger indirect radiative forcing.

Although the treatment of aerosol number in this experiment is closest of all MIRAGE experiments to the treatment in other models, the estimated indirect forcing is quite

Table 4. Number Mode Radius (When Aerosol Number is Diagnosed) and Geometric Standard Deviation σ_g for Each Aerosol Mode

	Aitken	Accumulation	Sea-Salt	Dust
Radius, μm	0.013	0.055	1.00	0.50
σ_g	1.6	1.8	2.0	1.8

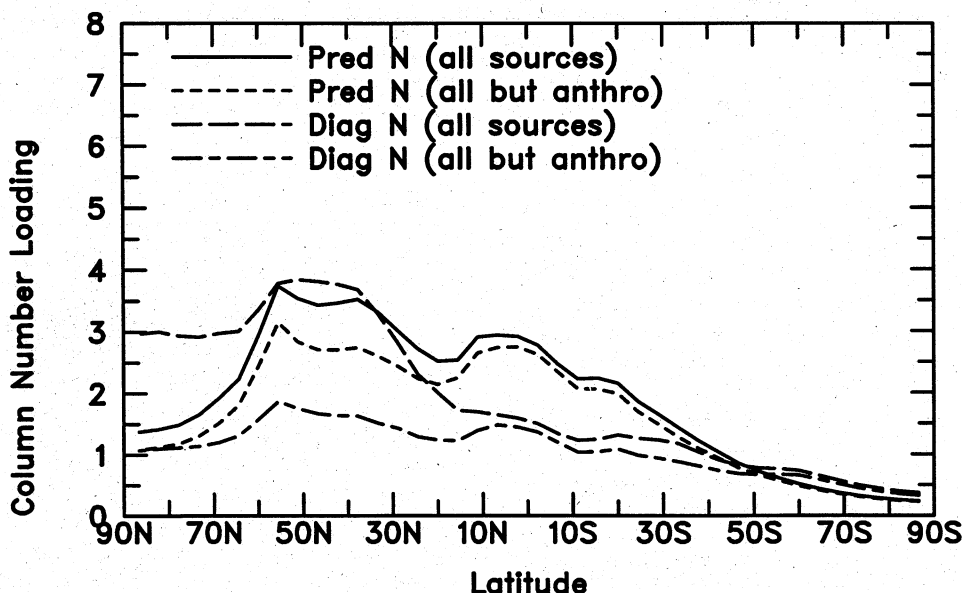


Figure 10. Annual and zonal mean column accumulation mode aerosol number concentration (10^{12} m^{-2}) simulated at R15 resolution with predicted aerosol number and all aerosol sources, predicted aerosol number and all sources except anthropogenic sulfur, diagnosed aerosol number and all aerosol sources, and diagnosed aerosol number and all sources except anthropogenic sulfur.

different. In particular, the indirect forcing estimate for externally mixed anthropogenic sulfate aerosol by ECHAM4 [Lohmann *et al.*, 2000] is about -0.1 W m^{-2} . Such a small estimate of indirect forcing is particularly surprising given the fact that the aerosol in the MIRAGE simulations without anthropogenic sulfate includes all present-day carbonaceous aerosol sources, but the ECHAM4 simulations used emissions of carbonaceous aerosol that are only 10% of present-day emissions. The much smaller “background” aerosol in the ECHAM4 simulations should produce a larger estimate of indirect forcing, rather than a much smaller estimate.

How can the two estimates of indirect forcing be reconciled? We have performed additional simulations with MIRAGE to reconcile the difference. In these simulations the carbonaceous aerosol emissions are set at 10% of present-day emissions. The aerosol size distributions are prescribed with mode radii and standard deviations identical to those used in the ECHAM4 PROG-ext simulations. The Lohmann *et al.* [2000] PROG-ext treatment of droplet nucleation is used. Most importantly, lower bounds of 300 cm^{-3} and 40 cm^{-3} are placed on the aerosol number and droplet number, respectively. The resulting estimate of indirect forcing is about -0.2 W m^{-2} , comparable to the Lohmann *et al.* [2000].

To understand the primary cause of the difference in the Lohmann *et al.* [2000] and MIRAGE estimates of indirect forcing, we have performed several additional experiments. First, we remove an inconsistency in the Lohmann *et al.* [2000] PROG-ext application of the Ghan *et al.* [1993] droplet nucleation parameterization, in which the activation parameter c was not scaled by a factor (4.8) that accounts for the dependence on size and composition; removing this inconsistency increases the MIRAGE estimate of the magnitude of the indirect forcing from -0.2 W m^{-2} to -0.3 W m^{-2} . Second, we apply less aggressive lower bounds of 100 and 10 cm^{-2} for aerosol number and droplet number concentration, respectively; the indirect forcing is -0.7 W m^{-2} . Third, we remove the lower bounds on aerosol number and droplet

number concentration; the indirect forcing increases to -2.7 W m^{-2} , comparable to the baseline MIRAGE estimate. These experiments suggest that the primary cause of the difference between the MIRAGE and the ECHAM4 estimates of indirect forcing are the lower bounds placed on aerosol number and droplet number concentrations in the ECHAM4 experiments. However, differences in the parameterization of droplet nucleation and in the prescribed aerosol size distribution (the larger size of sulfate particles in ECHAM4 yields a smaller indirect forcing and greater sensitivity to lower bounds on aerosol number) also contribute to the difference in the indirect forcing estimate.

4.5. Sensitivity to Relative Humidity

As noted by Ghan *et al.* [this issue (a)], MIRAGE simulates grid cell mean relative humidities near 100% more frequently than observed. The baseline simulations therefore use the ECMWF-analyzed relative humidity in the calculation of the aerosol water uptake and aerosol radiative properties. To test the sensitivity of the estimated radiative forcing to the treatment of relative humidity, we have repeated the baseline R15 simulation using the relative humidity simulated by MIRAGE to calculate the aerosol water uptake.

As might be expected, the indirect forcing is relatively insensitive to the aerosol water uptake, but the direct forcing is quite sensitive, increasing from -0.34 W m^{-2} with ECMWF relative humidity to -0.54 W m^{-2} with MIRAGE relative humidity. This increased forcing is driven by much larger increases in aerosol water content, with the anthropogenic change in global and annual mean column aerosol water increasing from 8.5 mg m^{-2} with ECMWF relative humidity to 27.8 mg m^{-2} with MIRAGE relative humidity. The global and annual mean column aerosol water simulated with all aerosol sources increases from 15.9 to 50.5 mg m^{-2} , a threefold increase. The global and annual mean aerosol optical depth simulated with all aerosol sources increases from 0.14 to 0.5, clearly unrealistic. Because of strong nonlinearity of aerosol

water uptake versus relative humidity, high relative humidities contribute strongly to the mean aerosol water content, even if their frequency is low. Thus an accurate frequency distribution for relative humidity is needed to accurately model aerosol water content.

5. Conclusions

In this study an integrated global aerosol and climate model was used to estimate the direct and indirect radiative forcing due to anthropogenic sulfate aerosols. It is distinguished from previous estimates of both direct and indirect forcing by its prognostic treatment of aerosol number and by its treatment of multiple aerosol modes.

The estimates of the forcing in the baseline experiment (-0.44 for direct and -1.7 W m^{-2} for indirect) are consistent with the broad range of estimates by other investigators. The indirect forcing has comparable contributions from the change in the droplet effective radius and from the response of the cloud liquid water content to the enhanced droplet number concentrations.

A variety of sensitivity experiments were conducted to provide information on the uncertainty of the radiative forcing estimate. The primary conclusions are as follows:

1. The sensitivity of both the direct and the indirect radiative forcing to model resolution is considerable, with the direct forcing being weaker and the indirect forcing being stronger at coarser horizontal resolution.

2. The indirect forcing with predicted droplet number is quite different from that with diagnosed droplet number. The difference is likely to be due to differences in the treatment of droplet formation in new versus aged clouds. Droplet number concentrations are much larger and more realistic in simulations with predicted droplet number.

3. The indirect forcing is rather sensitive to the parameterization of the droplet autoconversion, varying by 0.7 W m^{-2} .

4. The prediction of aerosol number yields an indirect forcing estimate that is 0.7 W m^{-2} smaller than the estimate with aerosol number diagnosed from aerosol mass and a prescribed aerosol size distribution. This reduction in the indirect forcing estimate is due to the ability of the model to distinguish between processes that primarily affect aerosol mass and those that primarily affect aerosol number. The influence of anthropogenic sulfate (a primarily secondary aerosol) on accumulation mode aerosol number (and hence droplet number) is consequently much lower if aerosol number is predicted rather than diagnosed. It is possible, however, that the treatment of aerosol nucleation in MIRAGE (based upon binary homogeneous nucleation theory) underestimates the influence of anthropogenic sulfate on accumulation mode number and hence droplet number.

5. The estimate of the indirect forcing by anthropogenic sulfate when aerosol number is diagnosed (-3.1 W m^{-2}) is much larger than the estimate (-0.1 W m^{-2}) by ECHAM4 [Lohmann *et al.*, 2000] for a comparable model configuration (PROG-ext-S). The difference in the estimates is largely due to the use of lower bounds on aerosol number and droplet number by Lohmann *et al.* [2000], but differences in the assumed aerosol size distribution and in the parameterization of droplet nucleation also contribute.

6. Direct forcing is quite sensitive to biases in relative humidity, particularly at relative humidities near 100%, because of the sensitivity of water uptake to relative humidity.

Estimating direct and particularly indirect forcing is difficult. Although much progress is documented in the literature in the recent years, much remains to be done before the estimates are reliable enough to base energy policy decisions upon. Necessary tasks for reducing uncertainty in estimates of aerosol radiative forcing include the following:

1. Emission estimates of both natural and anthropogenic aerosols and aerosol precursors must be improved. The uncertainty in some estimates is a factor of 2, averaged over the globe.

2. All important natural components of CCN must be treated in aerosol models used to estimate indirect radiative forcing. The organic component of the CCN is particularly poorly represented. The use of a lower bound on aerosol number when calculating droplet nucleation only covers a serious deficiency that must be corrected.

3. Subgrid variations in relative humidity, clouds, and cloud processes must be treated more realistically. MIRAGE treats subgrid variability in droplet nucleation but neglects subgrid variability in relative humidity (which is important for estimating direct effects [Haywood *et al.*, 1997]), in condensation, in autoconversion, and in collection processes. Adding treatments of such subgrid variability can reduce the dependence of the radiative forcing on the parameterization of water uptake and autoconversion.

4. Sulfate is but one of many anthropogenic aerosol components. Radiative forcing by all important anthropogenic aerosol needs to be estimated to distinguish between the radiative forcing of the present and the preindustrial climate.

5. Longer simulations than the 1-year simulation presented in this paper are needed to reduce the natural variability in the estimate of the radiative forcing. Other investigators have run 5 years, which is adequate given the other sources of uncertainty.

6. These relatively complex aerosol models need to be coupled with ocean models to estimate the climate response. Experiments with coupled atmosphere-ocean models have used much simpler and less reliable means for estimating the aerosol radiative forcing.

This list is hardly complete. One could easily add the usual list of uncertainties in the representation of clouds, etc.

Acknowledgments. This study was primarily supported by the NASA Earth Science Enterprise under contract NAS5-98072 and grants NAG5-8797 and NAG5-9531. Support was also provided by the U.S. Department of Energy Atmospheric Radiation Measurement Program, which is part of the DOE Biological and Environmental Research Program. The Pacific Northwest National Laboratory is operated for the DOE by Battelle Memorial Institute under contract DE-AC06-76RLO 1830.

References

- Albrecht, B. A., Aerosol cloud microphysics and fractional cloudiness, *Science*, **245**, 1227-1230, 1989.
- Arao, K., and Y. Ishizaka, Volume and mass of yellow sand dust from atmospheric turbidity, *J. Meteorol. Soc. Jpn.*, **64**, 79-93, 1986.
- Baker, M., and R. J. Charlson, Bistability of CCN concentrations and thermodynamics in the cloud-topped boundary layer, *Nature*, **345**, 142-145, 1990.
- Bolin, B., and R. J. Charlson, On the role of the tropospheric sulfur cycle in the shortwave radiative climate of the earth, *Ambio*, **5**, 47-54, 1976.
- Boucher, O., GCM estimate of the indirect aerosol forcing using satellite-retrieved cloud droplet effective radii, *J. Clim.*, **8**, 1403-1409, 1995.

- Boucher, O., and T. L. Anderson, General circulation model assessment of the sensitivity of direct climate forcing by anthropogenic sulfate aerosols to aerosol size and chemistry, *J. Geophys. Res.*, **100**, 26,117-26,134, 1995.
- Boucher, O., and U. Lohmann, The sulfate-CCN-cloud albedo effect: A sensitivity study with two general circulation models, *Tellus, Ser. B*, **47**, 281-300, 1995.
- Charlson, R. J., J. Langner, H. Rodhe, C. B. Leovy, and S. G. Warren, Perturbation of the northern hemisphere radiative balance by backscattering from anthropogenic sulfate aerosols, *Tellus, Ser. A*, **B**, **43**, 152-163, 1991.
- Charlson, R. J., S. E. Schwartz, J. M. Hales, R. D. Cess, J. A. Coakley Jr., J. E. Hansen, and D. J. Hofmann, Climate forcing by anthropogenic aerosols, *Science*, **255**, 423-430, 1992.
- Chin, M., and D. Jacob, Anthropogenic and natural contributions to tropospheric sulfate: A global model analysis, *J. Geophys. Res.*, **101**, 18,691-18,699, 1996.
- Chuang, C. C., J. E. Penner, K. E. Taylor, A. S. Grossman, and J. J. Walton, An assessment of the radiative effects of anthropogenic sulfate, *J. Geophys. Res.*, **102**, 3761-3778, 1997.
- Feichter, J., E. Kjellstrom, H. Rodhe, F. Dentener, J. Lelieveld, and G.-J. Roelofs, Simulation of the tropospheric sulfur cycle in a global climate model, *Atmos. Environ.*, **30**, 1693-1707, 1996.
- Feichter, J., U. Lohmann, and I. Schult, The atmospheric sulfur cycle in ECHAM-4 and its impact on the shortwave radiation, *Clim. Dyn.*, **13**, 235-246, 1997.
- Ghan, S. J., and R. C. Easter, Comments on "A limited-area-model case study of the effects of sub-grid-scale variations in relative humidity and cloud upon the direct radiative forcing of sulfate aerosol," *Geophys. Res. Lett.*, **25**, 1039-1040, 1998.
- Ghan, S. J., C. C. Chuang, and J. E. Penner, A parameterization of cloud droplet nucleation, Part I, Single aerosol type, *Atmos. Res.*, **30**, 197-222, 1993.
- Ghan, S. J., L. R. Leung, and Q. Hu, Application of cloud microphysics to NCAR CCM2, *J. Geophys. Res.*, **102**, 16,507-16,528, 1997a.
- Ghan, S. J., L. R. Leung, R. C. Easter, and H. Abdul-Razzak, Prediction of droplet number in a general circulation model, *J. Geophys. Res.*, **102**, 21,777-21,794, 1997b.
- Ghan, S. J., G. Guzman, and H. Abdul-Razzak, Competition between sea salt and sulfate particles as cloud condensation nuclei, *J. Atmos. Sci.*, **55**, 3340-3347, 1998.
- Ghan, S., N. Laulainen, R. Easter, R. Wagener, S. Nemesure, E. Chapman, Y. Zhang, and R. Leung, Evaluation of aerosol direct radiative forcing in MIRAGE, *J. Geophys. Res.*, this issue (a).
- Ghan, S. J., R. C. Easter, J. Hudson, and F.-M. Bréon, Evaluation of aerosol indirect radiative forcing in MIRAGE, *J. Geophys. Res.*, this issue (b).
- Graf, H.-F., J. Feichter, and B. Langmann, Volcanic sulfur emissions: Estimates of source strength and its contribution to the global sulfate distribution, *J. Geophys. Res.*, **102**, 10,727-10,738, 1997.
- Grant, K. E., C. C. Chuang, A. S. Grossman, and J. E. Penner, Modeling the spectral optical properties of ammonium sulfate and biomass burning aerosols: Parameterization of relative humidity effects and model results, *Atmos. Environ.*, **33**, 2603-2620, 1999.
- Haywood, J. M., and V. Ramaswamy, Global sensitivity studies of the direct radiative forcing due to anthropogenic sulfate and black carbon aerosols, *J. Geophys. Res.*, **103**, 6043-6058, 1998.
- Haywood, J. M., and K. P. Shine, The effect of anthropogenic sulfate and soot aerosol on the clear sky planetary radiation budget, *Geophys. Res. Lett.*, **22**, 603-606, 1995.
- Haywood, J. M., V. Ramaswamy, and L. J. Donner, A limited-area-model case study of the effects of sub-grid-scale variations in relative humidity and cloud upon the direct radiative forcing sulfate aerosol, *Geophys. Res. Lett.*, **24**, 143-146, 1997.
- Haywood, J. M., V. Ramaswamy, and B. J. Soden, Tropospheric aerosol climate forcing in clear-sky satellite observations over the oceans, *Science*, **283**, 1299-1303, 1999.
- Intergovernmental Panel on Climate Change (IPCC), *Climate Change 1994*, 339 pp., Cambridge Univ. Press, New York, 1995.
- Jones, A., and A. Slingo, Predicting cloud-droplet effective radius and indirect sulphate aerosol forcing using a general circulation model, *Q. J. R. Meteorol. Soc.*, **122**, 1573-1595, 1996.
- Jones, A., D. L. Roberts, and A. Slingo, A climate model study of indirect radiative forcing by anthropogenic sulphate aerosols, *Nature*, **370**, 450-453, 1994.
- Kiehl, J. T., and B. P. Briegleb, The relative roles of sulfate aerosols and greenhouse gases in climate forcing, *Science*, **260**, 311-314, 1993.
- Kiehl, J. T., T. L. Schneider, P. J. Rasch, M. C. Barth, and J. Wong, Radiative forcing due to sulfate aerosols from simulations with the NCAR community climate model, *J. Geophys. Res.*, **105**, 1441-1457, 2000.
- Koch, D., D. Jacob, I. Tegen, D. Rind, and M. Chin, Tropospheric sulfur simulation and sulfate direct radiative forcing in the GISS GCM, *J. Geophys. Res.*, **104**, 23,799-23,822, 1999.
- Lohmann, U., and J. Feichter, Impact of sulfate aerosols on albedo and lifetime of clouds: A sensitivity study with the ECHAM GCM, *J. Geophys. Res.*, **102**, 13,685-13,700, 1997.
- Lohmann, U., J. Feichter, J. E. Penner and R. Leaitch, Indirect effect of sulfate and carbonaceous aerosols: A mechanistic treatment, *J. Geophys. Res.*, **105**, 12,193-12,206, 2000.
- Myhre, G., F. Stordal, K. Restad, and I.S.A. Isaksen, Estimation of the direct radiative forcing due to sulfate and soot aerosols, *Tellus*, **50**, 463-477, 1998.
- National Research Council (NRC) Panel on Aerosol Radiative Forcing and Climate Change, 1996, in *Aerosol Radiative Forcing and Climate Change*, National Acad. Press, Washington, D.C., 1996.
- O'Dowd, C. D., M. H. Smith, I. E. Consterdine, and J. A. Lowe, Marine aerosol, sea-salt, and the marine sulfur cycle: A short review, *Atmos. Environ.*, **31**, 73-80, 1997.
- Penner, J. E., R. J. Charlson, J. M. Hales, N. S. Laulainen, R. Leifer, T. Novakov, J. Ogren, L. F. Radke, S. E. Schwartz, and L. Travis, Quantifying and minimizing uncertainty of climate forcing by anthropogenic aerosols, *Bull. Am. Meteorol. Soc.*, **75**, 375-400, 1994.
- Penner, J. E., C. C. Chuang, and K. Grant, Climate forcing by carbonaceous and sulfate aerosols, *Clim. Dyn.*, **14**, 839-851, 1998.
- Pham, M., J.-F. Müller, G. P. Brasseur, C. Granier, and G. Mégie, A three-dimensional study of the tropospheric sulfur cycle, *J. Geophys. Res.*, **100**, 26,061-26,092, 1995.
- Pham, M., J.-F. Müller, G. P. Brasseur, C. Granier, and G. Mégie, A 3D model study of the global sulphur cycle: Contributions of anthropogenic and biogenic sources, *Atmos. Environ.*, **30**, 1815-1822, 1996.
- Rotstaysn, L., Indirect forcing by anthropogenic aerosols: A global climate model calculation of the effective-radius and cloud-lifetime effects, *J. Geophys. Res.*, **104**, 9369-9380, 1999.
- Schult, I., J. Feichter, and W. F. Cooke, Effect of black carbon and sulfate aerosols on the global radiation budget, *J. Geophys. Res.*, **102**, 30,101-30,117, 1997.
- Tegen, I., A. A. Lacis, and I. Fung, The influence on climate forcing of mineral aerosols from disturbed soils, *Nature*, **380**, 419-422, 1996.
- Tegen, I., D. Koch, A. A. Lacis, and M. Sato, Trends in tropospheric aerosol loads and corresponding impact on direct radiative forcing between 1950 and 1990: A model study, *J. Geophys. Res.*, in press, 2000.
- Tripoli, G. J., and W. R. Cotton, A numerical investigation of several factors contributing to the observed variable intensity of deep convection over south Florida, *J. Appl. Meteorol.*, **19**, 1037-1063, 1980.
- Twomey, S., Aerosols, clouds, and radiation, *Atmos. Environ., Ser. A*, **25**, 2435-2442, 1991.
- van Dorland, R., F. J. Dentener, and J. Lelieveld, Radiative forcing due to tropospheric ozone and sulfate aerosols, *J. Geophys. Res.*, **102**, 28,079-28,100, 1997.
- Ziegler, C. L., Retrieval of thermal microphysical variables in observed convective storms, 1, Model development and preliminary testing, *J. Atmos. Sci.*, **42**, 1487-1509, 1985.
- E. G. Chapman, R. C. Easter, S. J. Ghan, N. S. Laulainen, L. R. Leung, and R. A. Zaveri, Pacific Northwest National Laboratory, Richland, WA 99352. (steve.ghan@pnl.gov)
- H. Abdul-Razzak, Texas A&M University-Kingsville, Kingsville, TX 78363.
- Y. Zhang, Atmospheric & Environmental Research, San Ramon, CA 94583
- R. D. Saylor, Georgia Institute of Technology, Atlanta, GA 30332.